Fermi National Accelerator Laboratory

FERMILAB-Conf-95/224-E
CDF

Observation of $B^+ \to J/\psi\pi^+$

F. Abe et al.
The CDF Collaboration

Fermi National Accelerator Laboratory
P.O. Box 500, Batavia, Illinois 60510

July 1995

Contributed to the *XVII International Symposium on Lepton-Photon Interactions*,
Beijing, China, August 10-15, 1995

Operated by Universities Research Association Inc. under Contract No. DE-AC02-76CHO3000 with the United States Department of Energy

Disclaimer

FERMILAB-CONF-95/224-E

Observation of $B^+ \to J/\psi\pi^+$

The CDF Collaboration

Abstract

We report on the observation of the Cabibbo-suppressed mode $B^+ \to J/\psi\pi^+$, with $J/\psi \to \mu^+\mu^-$. Further, we calculate the relative branching ratio, $BR(B^+ \to J/\psi\pi^+)/BR(B^+ \to J/\psi K^+)$ and find a value of $(4.9^{+1.9}_{-1.7} \pm 1.1)\%$.

1 Introduction

The $B^+ \to J/\psi\pi^+$ decay mode is Cabibbo-suppressed relative to $B^+ \to J/\psi K^+$[1]. Distinguishing $J/\psi\pi^+$ events from $J/\psi K^+$ events is difficult because the two modes overlap and CDF does not have particle identification in the momentum range of these events. A procedure to simultaneously fit $J/\psi\pi^+$ and $J/\psi K^+$ will be explained below. In addition, various checks on the $J/\psi\pi^+ \Big/ J/\psi K^+$ separation will be presented. The results reported will indicate a signal for $J/\psi\pi^+$, which has been previously reported by the CLEO Collaboration[2]. In addition, a measurement of the ratio of the branching ratios, $\frac{\mathrm{BR(B^+ \to J/\psi\pi^+)}}{\mathrm{BR(B^+ \to J/\psi K^+)}}$, will be determined.

The data for this analysis were collected at the CDF detector[3] during the 1992 Run-1a and ongoing 1994-1995 Run-1b at the Fermilab Tevatron. The data sample corresponds to an integrated luminosity of $\approx 63\mathrm{pb}^{-1}$ of $\bar{\mathrm{P}}\mathrm{P}$ collisions at a center-of-mass energy of 1.8 TeV.

2 Analysis

The $B^+ \to J/\psi K^+$ mode is fully reconstructed by considering all possible J/ψ and K^+ combinations. The J/ψ candidates were formed from $\mu^+\mu^-$ pairs which have a common vertex and invariant mass consistent with the J/ψ mass. All charged tracks were considered to be kaons. For the $B^+ \to J/\psi\pi^+$ mode, the charged tracks were assumed to be pions. The cuts used to optimize the signal were:

1. $|M_{\mu^+\mu^-} - M_{J/\psi}| < 2.5\sigma$
2. 2 or more tracks with links to the SVX tracking system
3. $\mathrm{CL}(\chi^2_{\mu^+\mu^-}) > 1\%$, to require that the muons form a good vertex.
4. $\mathrm{CL}(\chi^2_{J/\psi K^+}) > 1\%$, to require a good three-track vertex.
5. $\mathrm{P}_t(B^+) > 5.0$ GeV/c
6. $\mathrm{P}_t(K^+) > 1.25$ GeV/c
7. $\mathrm{L}_{xy} > 200\ \mu m$
8. $|\frac{\delta}{\sigma(\delta)}| > 1.5$, where δ is the impact parameter.

The mass distributions for the $J/\psi K^+$ and $J/\psi\pi^+$ combinations in the B^+ mass region are shown in Figures 1 and 2, respectively. The $J/\psi\pi^+$ figure shows a large excess below the B^+ mass due to $J/\psi K^+$ events in which the kaon was incorrectly assigned to be a pion.

The relative closeness of the mass of the $J/\psi K^+$ and $J/\psi\pi^+$ modes calls for a more elaborate fitting function than the standard Gaussian and linear background. We have used a likelihood function that fits the data to a $J/\psi K^+$ Gaussian, a $J/\psi\pi^+$ Gaussian and a linear background in $J/\psi K^+$. The mean mass and widths of the two Gaussians are held to be the same. The likelihood function, per entry, is given by

$$\mathcal{L}_i = \frac{N_{\psi K^+}}{\sqrt{2\pi}\sigma} e^{-\frac{(M_{\psi K^+} - M_{B^+})^2}{2\sigma^2}} + \frac{N_{\psi\pi^+}}{\sqrt{2\pi}\sigma} e^{-\frac{(M_{\psi\pi^+} - M_{B^+})^2}{2\sigma^2}} + P1(M_{\psi K^+})$$

where $P1(M_{\psi K^+})$ is a first order polynomial in ψK^+ mass given by

$$P1(M_{\psi K^+}) = aM_{\psi K^+} + b.$$

$N_{\psi K^+}$ is the number of ψK^+ events. $N_{\psi\pi^+}$ is the number of $\psi\pi^+$ events. M_{B^+} is the fitted B^+ meson mass. σ is the fitted Gaussian width.

The liklihood function, $L = \prod_{i=1}^{N} \mathcal{L}_i$, is maximized by varying $N_{\psi K^+}$, $N_{\psi\pi^+}$, M_{B^+} and σ. The results of this fit are given in the table below.

Parameter	Value
$\mathrm{N}_{\psi K^+}$	441 ± 17
$\mathrm{N}_{\psi\pi^+}$	25.1 ± 8.4
M_{B^+}	5.2786 ± 0.0008 GeV/c^2
σ	0.0139 ± 0.0008 GeV/c^2

From the fit, there are 441 ± 17 $B^+ \to J/\psi K^+$ events. The fitted B^+ mass and resolution are 5.2786 ± 0.0008 Gev/c^2 and 0.0139 ± 0.0008 Gev/c^2, respectively.

We find a signal of 25.1 ± 8.4 $J/\psi\pi^+$ events above a background of 25 events. A difficulty arises, however, in presenting this fit since it fits in two different spaces that do not transform simply. We have elected to show this as two separate plots, one for the ψK^+ peak and background, Figure 3, and one for the $\psi\pi^+$ peak and background, Figure 4. Each entry is weighted by its contribution to the ψK^+ Gaussian, the $\psi\pi^+$ Gaussian and the background. Each entry is plotted in both histograms with the appropriate weight.

The separation between $\psi\pi^+$ and ψK^+ is remarkable. The scatter plot in Figure 5 shows $M_{\psi\pi^+}$ against $\Delta M = M_{\psi K^+} - M_{\psi\pi^+}$. The horizontal lines are the 2.5σ lines for $\psi\pi^+$. The diagonal lines are the 2.5σ lines for the ψK^+ signal. This plot clearly demonstrates the excess of events in the B^+ mass region for $\psi\pi^+$ which are inconsistent with $B^+ \to J/\psi K^+$.

The relative efficiency accounts for kinematic differences of the two modes. The ratio of branching ratios is given by

$$\frac{\mathrm{BR}(B^+ \to J/\psi\pi^+)}{\mathrm{BR}(B^+ \to J/\psi K^+)} = \frac{\mathrm{N}_{\psi\pi^+}/\epsilon_{\psi\pi^+}}{\mathrm{N}_{\psi\mathrm{K}^+}/\epsilon_{\psi K^+}}$$

where $N_{\psi\pi^+}$ and $N_{\psi K^+}$ are the number of observed $\psi\pi^+$ and ψK^+ events, respectively, and $\epsilon_{\psi\pi^+}$ and $\epsilon_{\psi K^+}$ are the efficiencies of the cuts on these modes. We observe in the experiment $\frac{N_{\psi\pi^+}}{N_{\psi K^+}}$ and estimate the relative efficiency, $\epsilon_{rel} = \frac{\epsilon_{\psi\pi^+}}{\epsilon_{\psi K^+}} = 1.05 \pm 0.02$, from Monte Ca rlo.

Studying the difference in mass between the ψK^+ and $\psi\pi^+$ systems indicates that approximately 1% of the $\psi\pi^+$'s will be lost above the 5.6 GeV/c^2 cutoff in ψK^+. To correct for this, we have scaled the number of $\psi\pi^+$ by the reciprocal of the fraction of Monte Carlo events that fall in the fitting region. This correction if 1.009 ± 0.001.

With the relative efficiency calculated above, the relative branching ratio calculation is now straight-forward.

$$\frac{\mathrm{BR(B^+ \to J/\psi\pi^+)}}{\mathrm{BR(B^+ \to J/\psi K^+)}} = \frac{N^C_{J/\psi\pi^+}}{N_{J/\psi K^+}} / \frac{\epsilon_{J/\psi\pi^+}}{\epsilon_{J/\psi K^+}} = \frac{N_{J/\psi\pi^+}}{N_{J/\psi K^+}} / \epsilon_{rel} = (4.9^{+1.9}_{-1.7} \pm 1.1)\%$$

where $N^C_{J/\psi\pi^+}$ is the corrected number of $J/\psi\pi^+$ events. Various checks have been performed to confirm that the data and analysis techniques are behaving as expected. First, the background probability for ψK^+ is linear after removing the ψK^+ peak, as shown in Figure 8. Second, the Monte Carlo distributions of the $J/\psi K^+$ signal and backgro und are used to compare the expected ψK^+ distribution in $\psi\pi^+$ to data. In addition, $J/\psi\pi^+$ Monte Carlo events were added to explain the enhancement at the B^+ mass. The Monte Carlo plots are shown in Figures 9 and 10. Third, a check of the fitting procedure was performed. By randomly generating 450 ψK^+ events, and the expected background distributions, the fit procedure was tested on 1000 different data samples.

These samples had zero $\psi\pi^+$ events. The distribution of fitted $J/\psi\pi^+$ events for the fit procedure is shown in Figure 11. The candidate events and analysis procedure pass all the checks.

In conclusion, the evidence for observation of the $B^+ \to J/\psi\pi^+$ mode has been presented. CDF has 25.1 ± 8.4 $J/\psi\pi^+$ candidates. These events also are inconsistent with $B^+ \to J/\psi K^+$ candidates.

The relative branching ratio calculation was determined to be $(4.9^{+1.9}_{-1.7} \pm 1.1)\%$. The only other measurement of this quantity to date is $(4.3 \pm 2.3)\%$ by CLEO[2].

3 References

1 Throughout this paper, references to a specific charge state imply the charge-conjugate state as well.

2 CLEO Collaboration, Observation of $B \to \psi\pi$ Decays , ICHEP94 Ref GLS0393, July 13, 1994.

3 F. Abe, Nucl. Instru. Methods Phys. Res., Sect. A **271**, 387 (1988), and references therein.

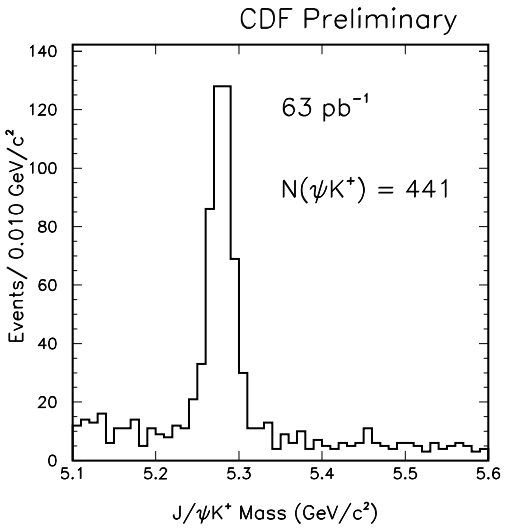

Figure 1: The figure shows the raw $J/\psi K^+$ mass distribution in the $B^+ \rightarrow J/\psi K^+$ mass window.

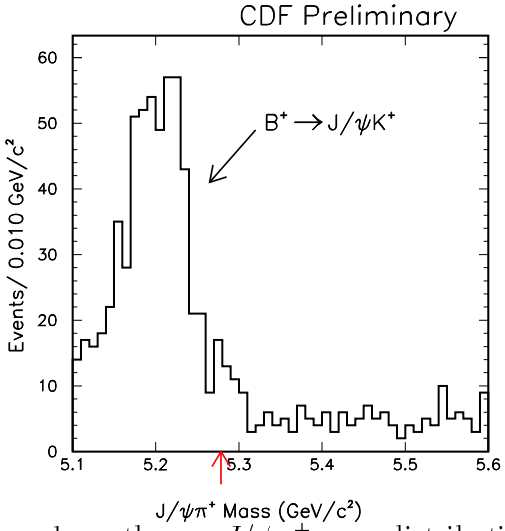

Figure 2: The figure shows the raw $J/\psi\pi^+$ mass distribution in the $B^+ \rightarrow J/\psi\pi^+$ mass window.

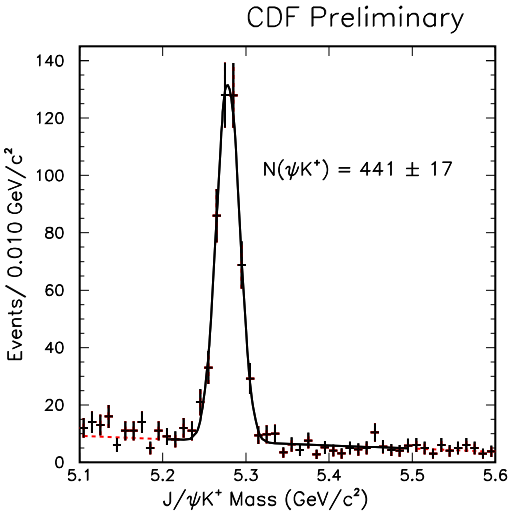

Figure 3: The fit to the $J/\psi K^+$ peak and linear background is shown in this figure. The $J/\psi\pi^+$ candidates have been removed by giving each event a weight equal to the probability that the event is not $B^+ \to J/\psi\pi^+$.

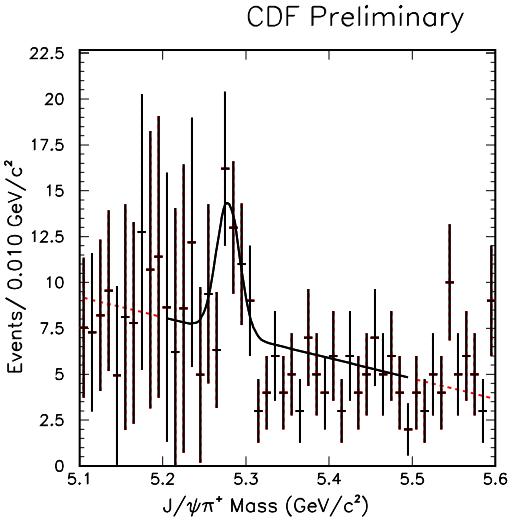

Figure 4: The fit to the $J/\psi\pi^+$ peak and linear background is shown in this figure. The $J/\psi K^+$ candidates have been removed by giving each event a weight equal to the probability that the event is not $B^+ \to J/\psi K^+$.

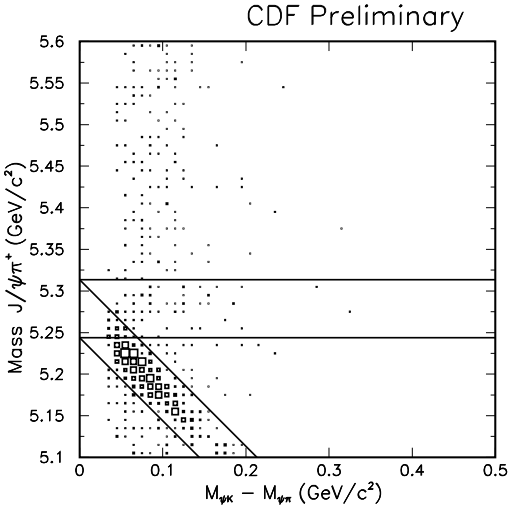

Figure 5: This figure shows the $J/\psi\pi^+$ mass distribution vs. the difference in mass for $J/\psi K^+$ and $J/\psi\pi^+$. The lines indicate the $\pm 2.5\sigma$ region for both $J/\psi\pi^+$ (horizontal) and $J/\psi K^+$ (diagonal). There are many $J/\psi\pi^+$ candidates outside the $J/\psi K^+$ signal region.

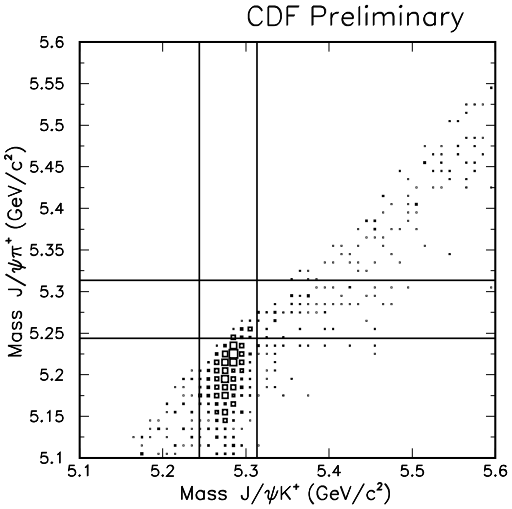

Figure 6: This figure shows the $J/\psi\pi^+$ mass vs. the $J/\psi K^+$ mass. The lines indicate the$\pm 2.5\sigma$ region for both $J/\psi\pi^+$ (horizontal) and $J/\psi K^+$ (vertical). There are many $J/\psi\pi^+$ candidates outside the $J/\psi K^+$ signal region.

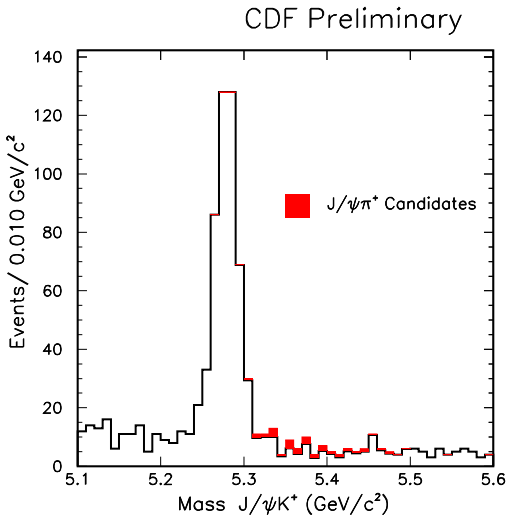

Figure 7: The raw $J/\psi K^+$ mass distribution is shown in the above figure. The $J/\psi\pi^+$ candidates are shaded to show their $J/\psi K^+$ mass. These events are shaded according to the probability, from the fit, that they are $J/\psi\pi^+$ events.

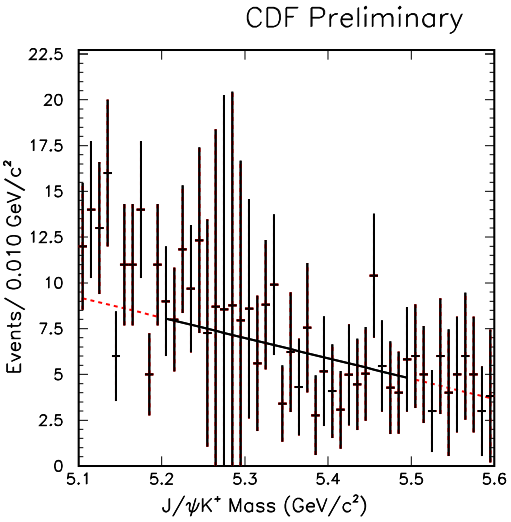

Figure 8: The figure shows the background distribution in the $J/\psi K^+$ mass window. Each event is weighted according to the probability that it is a background event. This removes the $B^+ \to J/\psi K^+$ events.

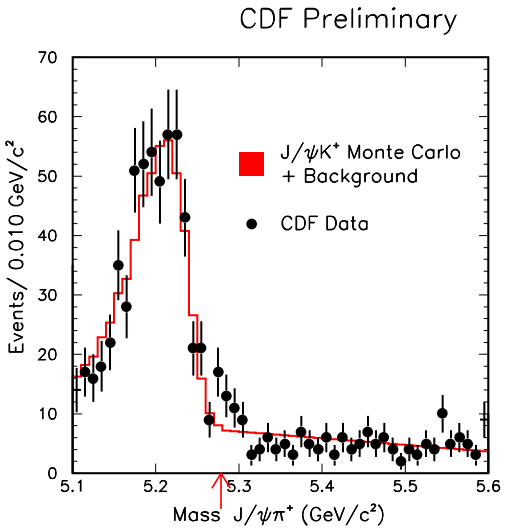

Figure 9: The above figure shows the fit with the superimposed Monte Carlo distribution for the $J/\psi K^+$ mode in the $J/\psi\pi^+$ signal region. The background is from the fit. The arrow indicates the mean B^+ mass, showing the excess unaccounted for by Monte Carlo and background.

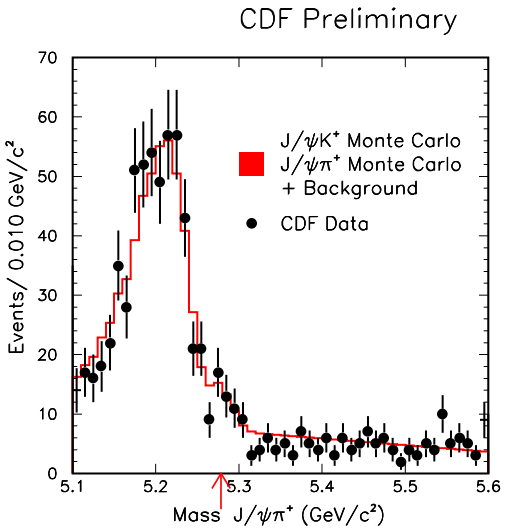

Figure 10: The above figure shows the fit with the superimposed Monte Carlo distribution for the $J/\psi K^+$ mode in the $J/\psi\pi^+$ signal region. The background is from the fit. In addition, a Gaussian at the B^+ mass models the $B^+ \to J/\psi\pi^+$ mode. The arrow indicates the mean B^+ mass.

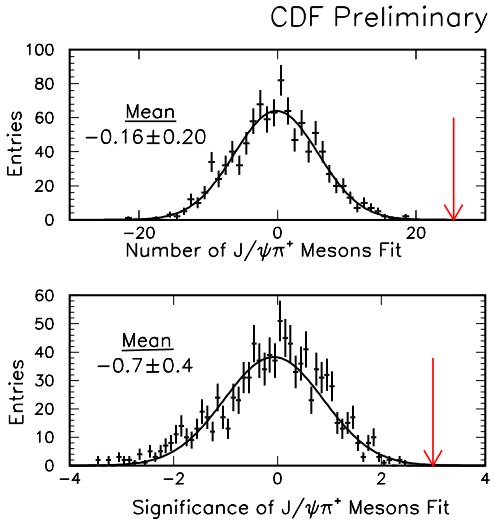

Figure 11: The top figure shows the number of $J/\psi\pi^+$ events found by the fitting procedure when tested on Monte Carlo data. There were no $J/\psi\pi^+$ events in the data that was fit, in agreement with the mean returned by the fit. The arrow indicates the number of $J/\psi\pi^+$ candidates fit on the real data. The lower figure, similarly, shows the distribution of the significance for Monte Carlo data. Again, the arrow indicates the real data.